RSC Advances

ROYAL SOCIETY OF CHEMISTRY

www.rsc.org/advances

Facile synthetic strategy of oleophilic zirconia nanoparticles allows preparation of highly stable thermo-conductive coolant.

Thadathil S. Sreeremya, Asha Krishnan, Lakshmi Narayan Satapathy and Swapankumar Ghosh*

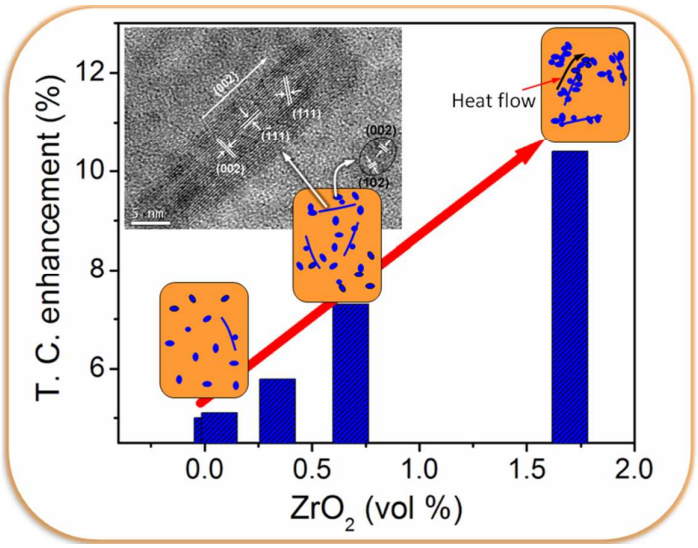

A simple one-step synthetic strategy was adopted for fabricating oil dispersable zirconia nanoparticles which produced remarkably stable nanofluid in transformer oil with enhanced thermal conductivity for cooling applications.

Journal Name

Dynamic Article Links ►

Cite this: DOI: 10.1039/c0xx00000x

www.rsc.org/xxxxxx

ARTICLE TYPE

Facile synthetic strategy of oleophilic zirconia nanoparticles allows preparation of highly stable thermo-conductive coolant.

Thadathil S. Sreeremya,[a] Asha Krishnan,[a] Lakshmi Narayan Satapathy[b] and Swapankumar Ghosh*[ac]

Received (in XXX, XXX) Xth XXXXXXXXX 20XX, Accepted Xth XXXXXXXXX 20XX
DOI: 10.1039/b000000x

We report a simple one-step method of fabricating monodisperse zirconium oxide nanoparticles by decomposing a zirconium oleate complex in a high boiling organic solvent. The X-ray and transmission electron microscopy on nanocrystals indicated the formation of monoclinic zirconia. The surfactant capped zirconia nanoparticles produced excellent dispersions in oils. The suitability of the nanofluids in heat transport was carefully investigated by measuring suspension stability, thermal conductivity and viscosity as a function of temperature. The effect of particle loading and temperature on the thermal conductivity of the oil based nanofluids and other promising features indicated potential application of ZrO_2 based nanofluids in heat transport sector. A thermal conductivity enhancement of ~10.3% was achieved with 1.7 vol% zirconia nanoparticle loading at room temperature. The TC of the nanofluids was remarkably higher than the same predicted by Maxwell and Hamilton-Crosser models.

Cite this: DOI: 10.1039/c0xx00000x

www.rsc.org/xxxxxx

ARTICLE TYPE

Introduction

Nanofluids are dispersions of nanoparticles (NPs) in a base fluid like water, oil, ethylene glycol,[1] etc. and have attracted widespread attention in the energy sector because of their enormous thermal conductivity (TC) enhancements that cannot be explained by existing theories/classical models.[2-3] Nanofluids for heat transport rely on the fact that solids have much higher thermal conductivity than common liquids and nanoparticulate solid addition into a base fluid substantially improves its effective TC.[4] High specific surface area of nanoparticles and the resultant higher suspension stability prevents clogging of the heat sink in cooling devices. Nanofluid coolants have potential applications in transportation,[5] electronics,[5-6] medical,[7] food, and many other process industries.[8] Engine oils, automatic transmission fluids, coolants, lubricants, and other synthetic high-temperature heat transfer fluids used in conventional IC engine radiators, engines, heating, ventilation and air-conditioning (HVAC) have inherently poor heat transfer properties. Heat transport driven failures are quite often in high voltage power transformers.[9] Due to the TC enhancement, oil based nanofluids provide efficient cooling which can extend the life of transformers.[9] A maximum of ~24% increase in thermal conductivity was reported for 2 vol% Cu nanoparticles dispersed in gear oil.[10] However, such nanofluids may cause arcing in high voltage transformer applications. The electric-insulating nature of transformer oils can be retained by dispersing insulating ceramic oxides such as zirconium oxide (commonly called as zirconia), while enhancing TC of the oils.[9] In addition, monoclinic form of zirconia has very high chemical and thermal stability. Water/ethylene glycol (EG) based nanofluids have already been extensively studied,[11] whereas, oil based fluids are not fully exploited for the heat transfer applications due to their inherent low thermal conductivity.

One of the major challenges which limit the widespread use of nanofluids is its poor stability against sedimentation.[4] In order to reduce their enhanced surface energy due to high surface area to volume ratio, NPs tend to cluster and form extended structures of linked NPs which in turn cause clogging of channels in the heat-transfer systems and a consequent decrease of the thermal conductivity. A key aspect in the synthesis of stable nanofluids is to overcome the high surface energy and to stabilize their thermodynamically unfavourable state. Steric stabilisation with the help of amphiphilic surfactants is the most widely used technique for preparing stable NP dispersions.[12-14] Oleic acid (OA) is one of the most widely employed surfactants for the synthesis of various metal, semiconductor, and metal oxide NPs. The carboxylic group binds to the positively charged NP surfaces and provide excellent steric hindrance due to its hydrocarbon tail projecting out in apolar solvents. Recent reports suggest that an organic route is preferred to aqueous methods for the preparation of stable nanofluids in apolar solvents, due to the greater control of particle size and polydispersity.[15] Solvothermal technique is reportedly one of the best methods for synthesis of organophilic zirconia NPs with good control of size[16] which requires high pressure and/or temperature, longer processing time, and additional safety protocols. Although the aqueous precipitation methods are simple, greener and inexpensive, they require multiple processing steps.[14] Solvothermal decomposition of an organic precursor on the other hand is a simple, one step method to fabricate monodispersed NPs with narrow size distribution.[15,17] There are only few reports regarding the synthesis of oleophilic zirconia nanostructures in recent years.[16,18-21] Most of these syntheses involve expensive alkoxide precursors and longer processing time.[18-21] Though these nanoparticles are reported to be dispersible in less viscous apolar solvents such as toluene, hexane etc., there is no mention about the stability of their suspensions, a prerequisite for most applications as fluid. However, the dispersion behavior of oleophilic zirconia in highly viscous solvents such as transformer oil is not yet studied.

Philip et al. reported the preparation and the temperature dependence of thermal conductivity of non aqueous magnetic nanofluids.[22] Choi et al. prepared transformer oil based nanofluids of Al_2O_3 and AIN NPs by a simple ball milling process.[9] Though zirconia has found widespread use in a wide range of applications due to its unique properties,[23] no efforts have so far been made to study the suitability of zirconia based nanofluids in transformer oil for cooling applications.

In this paper, we report a facile synthetic strategy for producing surface modified zirconia NPs from a zirconium oleate precursor by thermal decomposition in diphenyl ether in the presence of oleic acid as the capping agent. Stable oil-based nanofluids with varying zirconia content were prepared by dispersing these capped zirconia NP's in transformer oil. Thermal and rheological properties of these dispersions were studied. TC enhancements in zirconia nanofluids against NP loading and temperature of measurement are discussed. Zirconia based nanofluids with ~1.7% ZrO_2 demonstrated thermal conductivity enhancements of TO up to ~12.5%. An attempt is also made to propose the mechanism of thermal conductivity enhancements in the synthesized nanofluids.

Experimental Section

Preparation of zirconium-oleate

Zirconium oxychloride ($ZrOCl_2.8H_2O$, 99.99%) was procured from Indian Rare Earth Ltd. Oleic acid (99%) was supplied by Alfa Aesar, UK. Diphenyl ether (DPE, 99%) and oleyl amine (70%) were procured from Sigma Aldrich. Sodium hydroxide, ethanol and cyclohexane supplied by Merck, India were of analytical reagent grade. Double distilled water was used for the preparation of all aqueous solutions. Zirconium oxychloride (13.5 mmol) and sodium oleate (27 mmol) were dissolved in a mixture of 85 ml ethanol, 40 ml water and 100 ml cyclohexane. The mixture was heated to 80°C and was kept for 4 h.

Fig. 1 Optical photograph of as synthesized zirconium oleate complex

Cyclohexane containing the organic phase extract was collected and washed three times with 30 ml water. Excess solvent was evaporated off slowly at 80°C leaving a solid yellow residue as shown in Fig. 1.

Synthesis of ZrO_2 nanocrystals

In a typical synthesis, 13.3 mmol of the freshly synthesized zirconium oleate was dissolved in 40 ml DPE in a round bottom flask. To this, 16 mmol oleic acid and 16 mmol oleylamine were added and the reaction mixture was refluxed at its natural boiling point (~265 °C) for 4-10 h. As the reaction proceeded, the solution turned turbid brown, which indicated the formation of ZrO_2 nanocrystals. After natural cooling to room temperature, acetone was added to the reaction mixture to precipitate OA coated ZrO_2 NPs. The ZrO_2 precipitate was subsequently washed thoroughly with acetone several times and was dried in an air oven. The resulting precipitate could easily be dispersed in nonpolar solvents e.g., hexane, toluene etc. The capped NPs were dispersed in transformer oil (TO) by ultrasonication for about 10 minutes. EG as well as DPE were chosen as the refluxing media to prepare OA capped ZrO_2 NPs.

Instruments and characterization

The crystalline phase composition of the solid products were determined from the powder X-ray diffraction (XRD) patterns using a Philips X'PERT PRO diffractometer with Ni-filtered Cu $K\alpha_1$ radiation (λ = 1.5406 Å) in the 2θ range 20-100 degree at a scanning rate of 2º min^{-1} with a step size 0.04º. The morphology, average size of the ZrO_2 crystals and crystal structure were determined by high resolution transmission electron microscopy (HR-TEM) using a FEI Tecnai 30 G^2 S-Twin microscope operated at 300 kV and equipped with a Gatan CCD camera. A small amount of capped ZrO_2 was dispersed in toluene and ultrasonicated to get a stable suspension. TEM samples were prepared by dropping a micro-droplet of the suspension onto a 400 mesh copper grid and drying the excess solvent naturally. Size measurements for the colloidal zirconium oxide NPs in suspensions were performed at 25 ºC by photon correlation spectroscopy (PCS) on a Zetasizer 3000 HSA, Malvern Instruments, Worcestershire, UK using a 60 mW He-Ne laser operating at a wavelength of 633 nm with General Purpose algorithm with Dispersion Technology Software (v. 1.61) at 90º detection angle. Fourier transform infrared (FTIR) spectra of the as prepared products were recorded at room temperature using KBr (Sigma Aldrich, 99%) pellet method on a Nicolet Magna IR-560 spectrometer in the range 400 to 4000 cm^{-1} with average of 50 scans. The effective thermal conductivity (k_{eff}) of the nanofluids was measured using a thermal property analyzer (model KD2pro, Decagon Devices Inc., US) based on the transient hot wire method.[3,11,22] The sample vials with the thermal conductivity probe were immersed in a constant temperature water bath while measuring the thermal conductivity at different temperatures. The entire assembly was thermally insulated for avoiding temperature gradient and vibrations. The nanofluids were maintained at the desired temperature for a minimum of 10 min before conductivity measurements. The apparent viscosity of nanofluids was measured using a Physica rotational-type viscometer with the SC4–18 spindle (Rheolab® MC1vt2 rheometer) employing the concentric cylinder/bob and cup method. The measurement error was ±2% in all the cases. The colloidal stability of the nanofluids was monitored with a nephelometer (CL 52D, ELICO, India) as transmitted visible light through the fluid against of time.

Results and discussion

Zirconia NPs were prepared by the thermal decomposition of zirconium-oleate complex in high boiling solvents. The decomposition reaction was carried out by varying the solvent and reaction time. Sample details along with reaction conditions are provided in Table 1.

Table 1 Sample details along with reaction conditions

Sample code	Refluxing medium	Time of reflux (h)	Dispersibility in oil
ZEG4	EG	4	Nil
ZEG10	EG	10	Nil
ZDPE4	DPE	4	High
ZDPE7	DPE	7	High
ZDPE10	DPE	10	High

Apparently, no ZrO_2 crystal formation was observed by holding the reaction mixtures at temperatures below the boiling point of DPE solvent (265ºC). Metal carboxylates generally decompose on heating at ≥300°C to form metal oxide nanocrystals along with some by-products.[17] It was proposed that the decomposition reaction proceeds via the formation of free radicals from metal-oleates as shown in equations 1 and 2.[24]

$$M - OOCR \rightarrow \mathrm{M}^{\bullet} + \mathrm{R} - \mathrm{COO}^{\bullet} \quad (1)$$

$$M - OOCR \rightarrow \mathrm{MO}^{\bullet} + \mathrm{R} - \mathrm{CO}^{\bullet} \quad (2)$$

Subsequently, oleylamine assisted ionisation of oleic acid leads to the formation of ZrO_2 nanoparticles (NPs) with negatively charged oleate ions adsorbed on the surface and the core of the metal oxide remaining positively charged.[15,25] The reaction between the simultaneously produced Zr–$O^{\bullet}$ and $Zr^{\bullet}$ species forms Zr–O–Zr links which results in the formation of ZrO_2. However, a detailed and stoichiometric description of this chemical process has not yet been established.

Characterisation of surface modified nanocrystals

The phase composition of the capped zirconia nanocrystals

obtained by thermal decomposition of zirconium oleate in different solvents was determined by X-ray diffraction. The XRD profiles of zirconia crystals and FT-IR spectrum for ZPDE10 are shown in Fig. 2. The growth of zirconia crystals was found to increase with increasing the holding time at the reflux temperature.

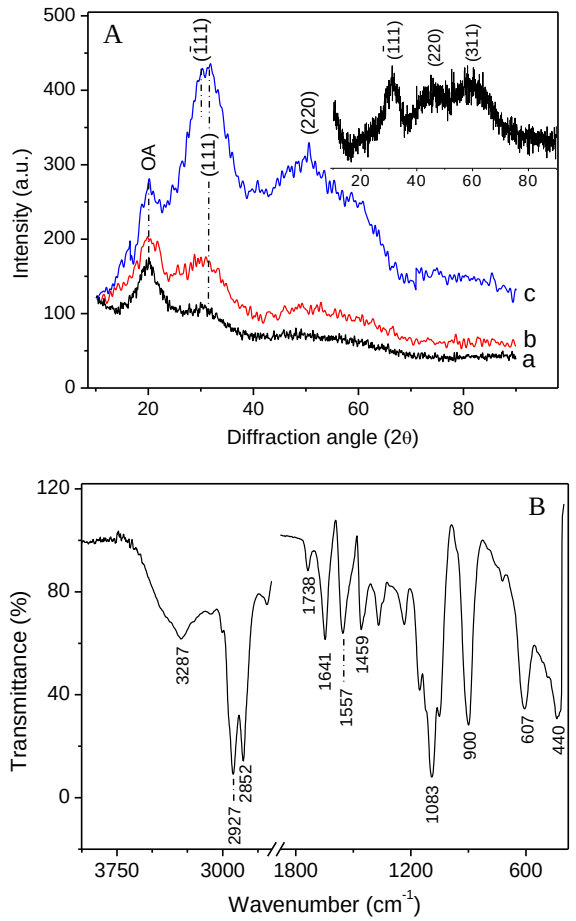

Fig. 2 (A) X-ray diffraction patterns of (a) ZDPE4, (b) ZDPE7, and (c) ZDPE10. The inset shows the XRD pattern of ZEG10 and (B) Fourier transform infrared spectra of ZDPE10.

All the X-ray profiles show a distinct diffraction peak at ~20° 2θ which is attributed to the presence of OA surfactant in the solids.[13] The relative intensity of this peak at ~20° 2θ to that of (111) reflection pertaining to monoclinic zirconia decreases with increase in reflux time indicating progressive formation of zirconia crystals. Four hour reflux treatment on Zr-oleate initiated the formation process of monoclinic zirconia crystals (ZDPE4) as indicated by the appearance of small humps corresponding to (111) and (220) crystal facets which grew sharper on further extending the reflux time to 10 h in ZDPE10. The profiles show three major finger print reflections from zirconia crystals of typical monoclinic structure with the space group: $P2_1/c$ (according to JCPDS card No. 830943) in ZDPE10 and ZEG10. Zirconia crystals grew larger to ~2.3±1 nm (D_{XRD}) with time through Ostwald ripening when the reflux time was extended to 10 h in ZDPE10 (>1 nm in ZDPE7). The dispersibility of NPs produced by reflux in DPE solvent (ZDPE) was relatively higher indicating efficient surfactant capping of the NPs than the same produced in EG solvent. This is attributed to the higher solubility of zirconium oleate complex in relatively less polar DPE solvent (dielectric constant, ε for DPE and EG are 3.9 and 37.7 respectively at 25°C). The FT-IR spectrum of ZDPE10 given in Fig. 2 provided evidence for the formation of OA capped zirconia nanocrystals. The C═O stretching vibration mode at 1738 cm^{-1} observed in capped *m*-ZrO_2 nanocrystals is attributed to the presence of OA in the material. The shift in the peak position from that of free oleic acid (1708 cm^{-1}) is due to the chemical interaction with the atoms on NP surfaces.[16] The bands in the range 2800-3000 cm^{-1} are the CH_2 and CH_3 symmetric and asymmetric stretching vibrations. The broad peak at ~3400 cm^{-1} is assigned to absorbed H_2O or –OH groups. The multiple peaks in the range 1000-1700 cm^{-1} can be assigned to the CH, –COO and H_2O modes or their mixtures. The strong peaks in the range 400-700 cm^{-1} are Zr-O vibration modes.[16] The peak at ~770 cm^{-1} is a typical feature for monoclinic zirconia.[26]

The size and morphology of the zirconia nanoparticles were examined by bright-field transmission electron microscopy (TEM) as shown in Fig. 3. The TEM image of ZDPE10 shows zirconia NPs of mostly ellipsoidal shape of average size ~4 nm along with scattered nanorods (inset of Fig. 3C) which is somewhat larger than the same calculated from X-ray peak broadening (2.3 nm). Crystal size determined from XRD profile using the Scherrer equation underestimates the grain size as it ignores broadening of the diffraction peaks due to the microstrain in the OA coated crystals.[14,27]

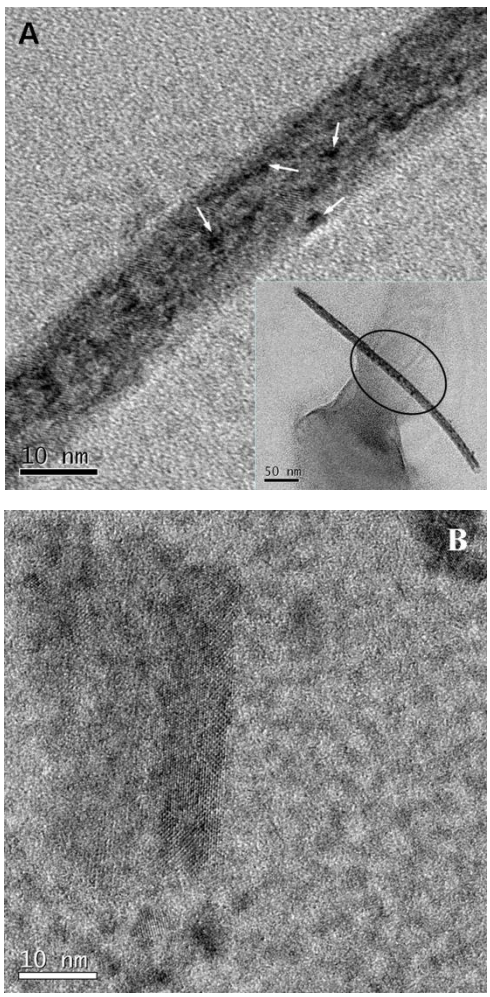

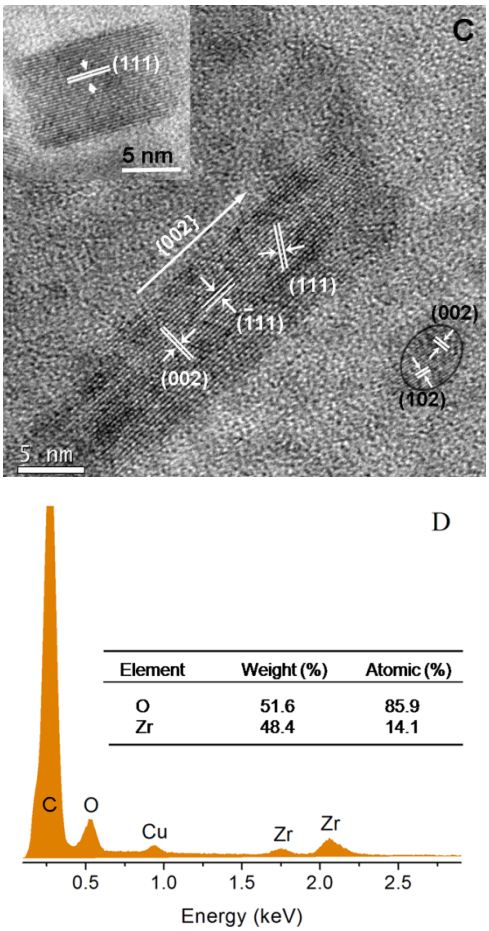

Fig. 3 TEM images (A and B) of monoclinic zirconia nanocrystals (ZDPE10), (C) High-resolution TEM image of ZDPE10 of mixed morphology, and (D) EDS spectrum of ZDPE10 with the elemental analysis shown as inset.

The formation of well crystallised zirconia nanocrystals in ZDPE10 (10 h refluxing in DPE) is evident from the HR-TEM images provided in Fig. 3. The predominant (111), (111), and (002) lattice fringes with corresponding interplanar spacing of 0.31, 0.28 and 0.26 nm respectively, were observed in the HR-TEM image of the nanorods and NPs confirming that zirconia produced has monoclinic structure (JCPDS card No. 830943).[28] A small number of NPs are sticking onto the surface of the nanorods as indicated by arrow marks in Fig. 3A. Detailed analysis of the images reveals that the nanoparticles consist of approximately 87% rods and 13% ellipsoidal particles by volume (or mass). The nanorods have an average length of ~300 nm and diameter ~8 nm. During the longer duration of reflux treatment (>7 h) the ellipsoidal crystals have shown 1D growth in the [002] direction. The atomic ratio of zirconium to oxygen obtained from the EDS spectrum (Fig. 3D) confirms that the oxygen content in the sample is slightly in excess of the stoichiometric requirement for ZrO_2 due to the presence of chemisorbed oleic acid in the sample.

The size of ZrO_2 NPs (ZDPE10) in toluene suspension was measured by photon correlation spectroscopy (PCS) and the size (hydrodynamic diameter) distribution is shown in Fig. 4. The light scattering data shows that ZDPE10 contains colloidal ZrO_2 particles in the size range 5-20 nm with an average hydrodynamic diameter (D_{PCS}) of 9.8 nm which is the weighted average of few nanorods of equivalent spherical diameter of ~32 nm and the majority spheroidal particles of hydrodynamic diameter of ~6 nm with 4 nm core.[14]

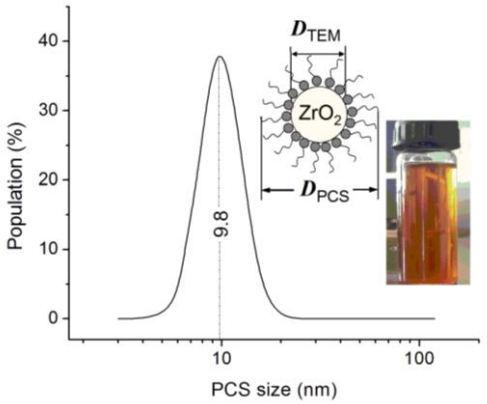

Fig. 4 Particle size distribution (number) of capped ZDPE10 suspension in toluene as measured by photon scattering technique. Image of transparent colloidal dispersion of ZrO_2 in TO is also shown as inset.

The polydispersity index (PDI) for the distribution is 0.35 which indicates that the distribution is relatively wide.

Rheological Properties of Nanofluids

As nanofluids for heat transport are used under continuous-flow conditions, the rheological properties play a vital role in determining its suitability in real applications. NPs suspended in nonpolar liquids, such as mineral oil and other hydrocarbons, are known to increase the viscosity of the fluid by forming transient interparticle linkages arising out of the net attractive forces among the particles.[11] The flow behaviour of zirconia based nanofluids as measured by viscosity is shown in Fig. 5. Suspensions containing ≤0.7 vol% zirconia NPs displayed almost same trend as that of the base fluid. A non-newtonian behaviour at low shear rate was already reported for oil.[29] Newtonian behaviour was observed for nanofluids above the shear rate of 200 s^{-1} with negligible effect on the viscosity against shear rate as there were no significant interactions among the particles. This is due to the large separation among the particles in lower concentration of ZrO_2.

On increasing the ZrO_2 content to 1.7 vol%, shear-thinning was observed at low shear rates, followed by ideal viscous flow behaviour.

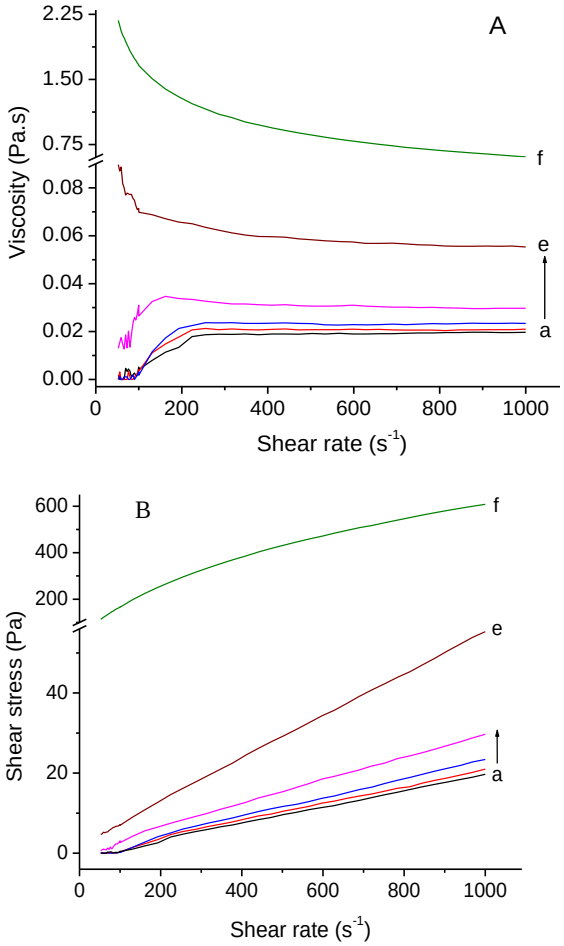

Fig. 5 Flow curves (A-viscosity and B-shear stress) for transformer oil based nanofluids with a) pure oil, b) 0.03, c) 0.07, d) 0.34, e) 0.68, and f) 1.7 vol% ZDPE10.

The suspensions transformed into viscous gel-like fluid forming three-dimensional network on increasing the zirconia NP loading Shear force is responsible for the disintegration of the gel structure, resulting in a decrease in viscosity on further increase in shear force.[30]

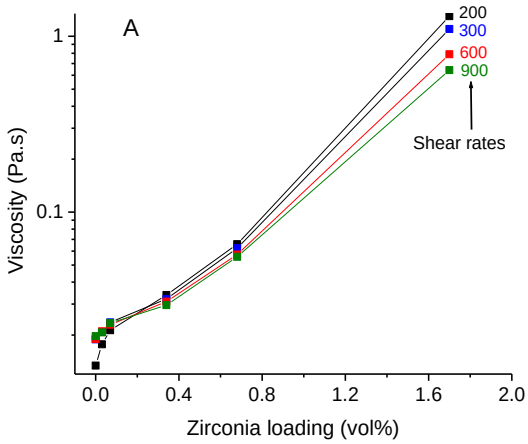

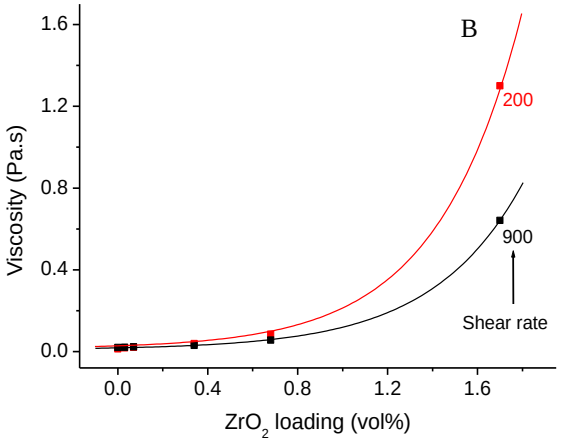

Fig. 6 (A) Profiles and (B) fits on viscosity data for TO based nanofluids as a function of ZDPE10 loading at different shear rates.

Breaking of the gel-structure decreases the interaction forces among the particles lowering the flow resistance.[31] The displaying of the curves of figure 2 can be explained as follow. For detailed analysis, the viscosity of nanofluids as a function of zirconia loading at few selected shear rates is shown in Fig. 6 which demonstrates nonlinear increase in viscosity of TO with increase in NP loading. The viscous suspensions with 0.68 and 1.7 vol% ZDPE10 (layers 'e' and 'f' in Fig. 5B) clearly behave as a yield stress fluid as the shear stress differs to zero when the shear rate vanishes. The increase in viscosity is nonlinear with zirconia NP loading which can be fit into the following exponential growth equation (3):

$$v = a(e^{bx} + 1) \quad (3)$$

where v is the viscosity, x is the NP (ZDPE10) loading in vol% and the constants a = 0.0103 and 0.0091, b = 2.844 and 2.497 at 200 and 900 shear rates respectively. The effect of temperature on viscosity of nanofluids is shown graphically in Fig. 7.

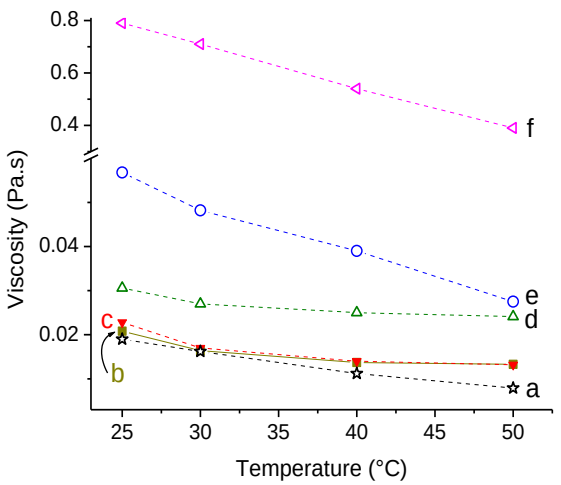

Fig. 7 The variation of viscosity with increase in temperature for a) pure oil, b) 0.03, c) 0.07, d) 0.34, e) 0.68 and f) 1.7 vol% ZDPE10 nanofluid

Viscosity of liquids is strongly temperature dependent and it decreases in most of the liquids with increase in temperature.[32] The average kinetic energy of the molecules in a liquid increases

with increase in temperature of the liquid.[30] The increased kinetic energy of the molecules overcomes the attractive forces easily that tend to hold the molecules together. The viscosity of base oil and nanofluids was found to decrease with increase in temperature. This trend was more apparent in the case of viscous fluids with nanoparticle concentration ≥0.68 vol%. The breaking of the gel structure during shearing[30] and increase in activation energy with temperature might have played the key roles here. The viscosity of fluid containing 1.7 vol% ZDPE10 in TO decreased almost linearly from initial ~0.8 Pa.s at 25 °C to ~0.4 Pa.s at 50 °C (Fig. 7). This phenomenon is typical to a liquid without any suspended NPs which could possibly imply that the nanofluids are indeed true colloidal suspensions.

Stability of nanofluids

In addition to thermal conductivity, the most important property which decides the suitability of a nanofluid in industrial heat transport applications is its suspension stability. The zirconia NPs dispersed in transformer oil was apparently stable at room temperature for months without changing their appearance, and detectable precipitation. The stability was ensured by performing ageing studies which includes measurement of thermal conductivity and turbidity at constant temperature of 25 °C over a period of six months and are shown in Fig. 8.[33-34]

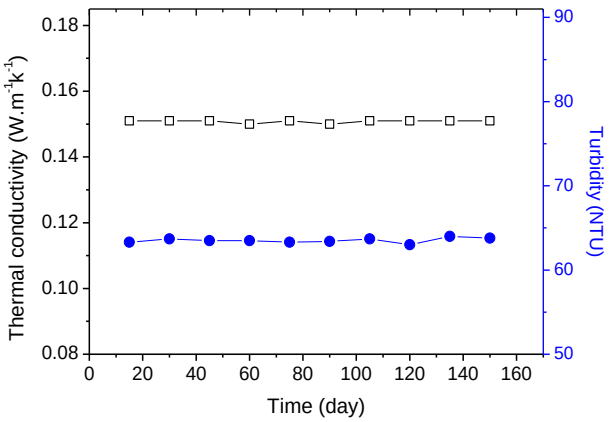

Fig. 8 Stability of nanofluids as measured by thermal conductivity (empty squares) and turbidity (filled circles) of 1.7 vol% ZDPE10 as a function of time.

The turbidity and thermal conductivity for the base transformer oil was measured as 1 NTU and 0.137 $Wm^{-1}K^{-1}$ respectively. The effective thermal conductivity remained more or less constant during the long period of measurement. The turbidity remained constant during the measurement period. The stability data once again corroborates the findings shown in Fig. 9.

Thermal Conductivity of Nanofluids

The thermal conductivity enhancement of zirconia nanofluids (k_{eff}) is calculated using equation 4.

$$k_{eff} = \frac{(k_{nf} - k_0)}{k_0} \times 100 \quad (4)$$

where k_{nf} and k_0 are the thermal conductivities of nanofluid and base fluid respectively. Fig. 9 shows the effective thermal conductivity enhancements in ZrO_2 nanofluids as a function of volume fraction of ZDPE10 as well as fluid temperatures. As expected, the thermal conductivity of all the nanofluids was higher than that of its base fluid and increased almost linearly with increase in NPs loading. Most of the existing theoretical models rely on the thermal conductivity of the solid and the liquid and their relative volume fraction, not on the particle size and the interface between the particles and the fluid.[35] The thermal conductivity data was fitted to Maxwell model[36] (Eq. (5)) which predicts TC enhancements in nanofluids with spherical particles as well as Hamilton-Crosser model[34] (Eq. (6) which allows TC calculation considering the shape factor of NPs in addition to their individual thermal conductivities and are shown in Fig. 9.

$$\frac{k_{eff}}{k_0} = 1 + \frac{3\Phi(k_p - k_0)}{[2k_0 + k_p - \Phi(k_p - k_o)]} \quad (5)$$

$$\frac{k_{eff}}{k_0} = \frac{k_p + (n-1)k_0 + (n-1)(k_p - k_0)\Phi}{k_p + (n-1)k_0 - (k_p - k_0)\Phi} \quad (6)$$

where k_{eff}, k_p, and k_0 are thermal conductivities of the nanofluids, solid particles, and the base fluid respectively, and φ is the nanoparticle volume fraction. The empirical shape factor 'n' calculated based on the average dimensions of particles from HR-TEM was found to be 4.5.[36]

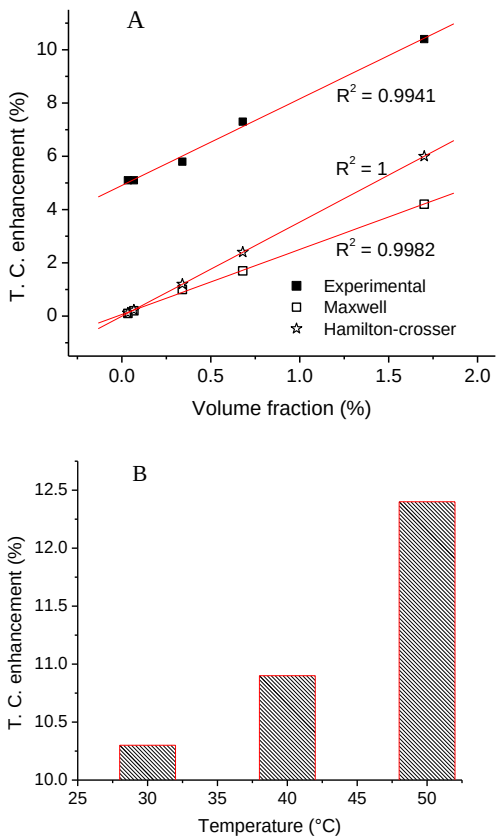

Fig. 9 (A) Thermal conductivity of nanofluids as a function zirconia NP (ZDPE10) loading in transformer oil measured at 25 °C, (B) The variation

in thermal conductivity of 1.7 vol% zirconia fluid at three different temperatures (30, 40, and 50 °C). The standard deviation in the *k* measurement was within ±5%.

The TC values obtained are remarkably higher than the ones predicted by both these models and are closer to the Hamilton-Crosser predictions. The mixed crystal morphology of NPs observed under TEM (Fig. 3) supports this prediction. A 5.1% increase in thermal conductivity was observed with 0.03 vol% ZrO_2 NP in TO which further increased to ~7.3% when the loading was increased to 0.68 vol%. The nanofluid with highest ZrO_2 loading in this study (1.7 vol%) resulted in a 10.3% increase in thermal conductivity (Fig. 9). Nanofluids with <1 vol% NP loading have shown marginal enhancements in thermal conductivity. Most of the reports on heat transport fluids attributed Brownian motion as the main mechanism of heat transfer in nanofluid systems.[37-40] In the present investigation, we propose that the heat transfer is driven via particle-particle contact, in addition to Brownian motion which is less prominent in the case of gel-like suspensions (Scheme 1). Thermal conductivity of 1.7 vol% ZDPE10 nanofluid increased from an initial ~10.35% measured at 30 °C to ~12.4% when the temperature of measurement was increased to 50 °C (Fig. 9B). Nanofluids with 0.03 and 0.34 vol% have shown 7.3 and 10.4% enhancement in TC at 50 °C. An increase in temperature leads to enhancement in Brownian component of the particles, which improves the rate of heat transfer assuming the transport through contact mode remains constant.

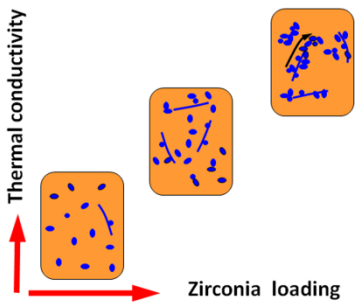

Scheme 1 Enhanced TC with higher particle-particle contact in fluids from low to high loading of ZDPE10 NPs.

The Brownian motion of the particles does not enhance the mass transport, but it increases the convective flows because of an increase in the nanoscale stirring of the fluid.[22] The thermal conductivity of the nanofluids depends not only on the volume fraction, but also on the shape of the particles.[41] Rod-shaped particles are reported to be more efficient in heat transfer compared to the spherical counterparts.[9] Zirconia being a low thermal conductivity material (TC ~2 $W.m^{-1}k^{-1}$), has shown reasonably high ~10.3% enhancement in thermal conductivity at 1.7 vol% loading. This is attributed to i) appreciable fraction of small particles, ii) rod like/elongated morphology of remaining particles, and iii) compatibility of capped particles with TO. However, the viscosity of NPs in oil suspensions increases almost exponentially with increase in NP loading creating a virtual limit.

Evaluation of efficiency of nanofluids

The effectiveness of various liquid coolants depends on the flow mode (laminar/turbulent) and can be estimated based on fluid dynamics equations. In the simple case of fully developed laminar flow, use of nanofluid will be beneficial if the increase in the viscosity is less than four times the increase in thermal conductivity,[42]

$$\frac{\eta}{\eta_0} = 1 + C_\eta\,, \qquad \frac{k}{k_f} = 1 + C_k\,, \qquad \frac{C_\eta}{C_k} < 4$$

where C_η and C_k are viscosity and thermal conductivity enhancement coefficients, determined from experimental viscosity and thermal conductivity ratios. The C_μ/C_k value for 0.03, 0.34 and 1.7 vol% nanofluid at a shear rate of 1000 s^{-1} is shown in Table 2.

Table 2 Ratio of viscosity enhancement coefficient to thermal conductivity enhancement coefficient as a function of vol% of NPs and temperature.

Vol%	C_μ/C_k	
	25 °C	50 °C
0.03	3	1.2
0.34	8.6	5.1
1.7	292	233

It is clear that the ratio of viscosity enhancement coefficient to thermal conductivity enhancement coefficient is less than 4 at 25° and 50 °C for 0.03 vol% whereas the value crossed 4 when the nanoparticle concentration increased to 0.34%. The ratio for 0.03 vol% is comparable to the value reported by Estelle et al. for carbon nanotube based fluid at 40 °C and is much less than that reported by Timofeeva et al. for cylindrical alumina nanoparticles.[43-44] Timofeeva et al. ascribed this high value to the high viscosity offered by cylindrical particles.[44] In our case the mixed morphology of particles and few nanorods offered less resistance to flow at low particle concentration and produced reasonable enhancement in TC rendering the nanofluids efficient. Nanofluids with reasonably low viscosity (0.03 vol%) offer better performance than nanofluids with highest thermal conductivity and high viscosity (1.7 vol%) because of the high pumping power required for viscous fluid.[22] This means that though the thermal conductivity enhances with increase in nanoparticle concentration, its effect is partly nullified by the viscosity enhancement of the nanofluids. At all concentrations the C_μ/C_k value was found to decrease with increase in temperature indicating that the nanofluid's efficiency increases with increase in temperature.[43] This simple method is amenable to large-scale production of nanofluids.

Conclusions

A comparatively simple method for preparing well-dispersed zirconia NPs in transformer oil was presented in this work. Surface modified zirconia NPs of elongated/rod like morphology have been successfully synthesized by the thermolysis of its oleate precursor. The surface functionalized nanocrystals are ideal for nanofluid preparation as they offer long term stability over six months. The reasonably high thermal conductivity offered by zirconia nanofluid can be attributed to the elongated

morphology of the nanocrystals. The nanofluid loaded with 1.7 vol% NPs has shown 10.3% enhancement in thermal conductivity with respect to that of base oil. The promising TC enhancements, long-term stability, good flow characteristics enable the zirconia NP-transformer oil nanofluids to have applications in engineering fields and thermal energy management systems.

Acknowledgments

This work was supported by the Bharat Heavy Electricals Ltd., Bangalore, India. The authors are grateful to the Director, CSIR-National Institute for Interdisciplinary Science & Technology (NIIST) for providing the necessary facilities for the work and CSIR-Central Glass & Ceramic Research Institute for continuing the same. Authors thank the Department of Science & Technology (DST) and CSIR, India for providing HR-TEM facility to NIIST. Author (TSS) thanks BHEL, India, and CSIR for the fellowships and (AK) acknowledges CSIR for the CSIR-UGC SRF fellowship.

Notes and references

[a] *Material Science and Technology Division, National Institute for Interdisciplinary Science & Technology (NIIST), Council of Scientific & Industrial Research (CSIR)*
Trivandrum-695019, India

[b] *CTI, Corporate R & D, BHEL*
Malleswaram Complex,
Bangalore-560012, India

[c] *ACTC Div, Central Glass & Ceramic Research Institute, CSIR, 196 Raja S. C. Mullick Road, Kolkata-700 032, India.*
E-mail: swapankumar.ghosh2@mail.dcu.ie
Fax: +91-33-24730957; Tel: +91-33-23223546
Homepage: http://www.cgcri.res.in

1 T. T. Baby and S. Ramaprabhu, *J. Mater. Chem.*, 2011, **21,** 9702.
2 K. V. Wong and O. De Leon, *Adv. Mech. Eng.*, 2010,
3 B. Wang, J. Hao and H. Li, *Dalton Trans.*, 2013, **42,** 5866.
4 X.-Q. Wang and A. S. Mujumdar, *Int. J. Therm. Sci.*, 2007, **46,** 1.
5 V. Sridhara and L. N. Satapathy, *Nanoscale Res. Lett.*, 2011, **6,** 1.
6 I. Manna, *J. Indian Inst. Sci. A Eng*, 2009, **89:1,** 21.
7 L. Cheng, *Recent Patents on Engineering*, 2009, **3,** 1.
8 D. M. F. W. Yu, J. L. Routbort, S. U. S. Choi, *Heat Trans. Eng.*, 2008, **29,** 432.
9 C. Choi, H. S. Yoo and J. M. Oh, *Curr. Appl. Phys.*, 2008, **8,** 710.
10 M. Kole and T. K. Dey, *Appl. Therm. Eng.*, 2013, **56,** 45.
11 S. S. Botha, P. Ndungu and B. J. Bladergroen, *Ind. Eng. Chem. Res.*, 2011, **50,** 3071.
12 M. T. Lopez-Lopez, J. D. G. Duran, A. Delgado and F. Gonzalez-Caballero, *J. Colloid Interf. Sci.*, 2005, **291,** 144.
13 A. Ahniyaz, Y. Sakamoto and L. Bergstrom, *Cryst. Growth Des.*, 2008, **8,** 1798.
14 T. S. Sreeremya, K. M. Thulasi, A. Krishnan and S. Ghosh, *Ind. Eng. Chem. Res.*, 2012, **51,** 318.
15 A. Krishnan, T. S. Sreeremya, E. Murray and S. Ghosh, *J. Colloid Interf. Sci.*, 2013, **389,** 16.
16 X. Xu and X. Wang, *Nano Res.*, 2009, **2,** 891.
17 T. D. Schladt, T. Graf and W. Tremel, *Chem. Mater.*, 2009, **21,** 3183.
18 J. Joo, T. Yu, Y. W. Kim, H. M. Park, F. X. Wu, J. Z. Zhang and T. Hyeon, *J. Am. Chem. Soc.*, 2003, **125,** 6553.
19 M. Mizuno, Y. Sasaki, S. Lee and H. Katakura, *Langmuir*, 2006, **22,** 7137.
20 G. Garnweitner, L. M. Goldenberg, O. V. Sakhno, M. Antonietti, M. Niederberger and J. Stumpe, *Small*, 2007, **3,** 1626.
21 T. A. C. a. G. Garnweitner, *CrystEnggComm*, 2014, **16,** 3366.
22 P. D. Shima, J. Philip and B. Raj, *J. Phys. Chem.C*, 2010, **114,** 18825.
23 P. Tartaj, O. Bomati-Miguel, A. F. Rebolledo and T. Valdes-Solis, *J. Mater. Chem.*, 2007, **17,** 1958.
24 F. Kenfack and H. Langbein, *Thermochim. Acta*, 2005, **426,** 61.
25 M. Klokkenburg, J. Hilhorst and B. H. Erne, *Vib. Spectrosc.* 2007, **43,** 243.
26 E. F. Lopez, V. S. Escribano, M. Panizza, M. M. Carnasciali and G. Busca, *J. Mater. Chem.*, 2001, **11,** 1891.
27 S. C. Tjong and H. Chen, *Mater. Sci. Eng. R*, 2004, **45,** 1.
28 M. Ambrosi, E. Fratini, P. Canton, S. Dankesreiter and P. Baglioni, *J. Mater. Chem.*, 2012, **22,** 23497.
29 M. T. Jamal-Abad, M. Dehghan, S. Saedodin, M. S. Valipour and A. Zamzamian, *J. Heat Mass Transf. Res.*, 2014, **1, 17.**
30 P. Estellé, S. Halelfadl, N. Doner and T. Maré, *Curr. Nanosci.*, 2013, **9**, 225.
31 S. K. Chen, G. Oye and J. Sjoblom, *J. Disper. Sci. Technol.*, 2005, **26,** 791.
32 P. G. Wright, *Phys. Educ.*, 1977, 323.
33 D. Kim, Y. Hwang, S. I. Cheong, J. K. Lee, D. Hong, S. Moon, J. E. Lee and S. H. Kim, *J. Nanopart. Res.*, 2008, **10,** 1121.
34 M. Janus, M. Inagaki, B. Tryba, M. Toyoda and A. W. Morawski, *Appl. Catal. B-Environ.*, 2006, **63,** 272.
35 Q. Z. Xue, *Phys. Lett. A*, 2003, **307,** 313.
34 36 D. Singh, E. Timofeeva, W. Yu, J. Routbort, D. France, D. Smith and J. M. Lopez-Cepero, *J. Appl. Phys.*, 2009, **105,**
37 S. P. Jang and S. U. S. Choi, *Appl. Phys. Lett.*, 2004, **84,** 4316.
38 D. Li, B. Hong, W. Fang, Y. Guo and R. Lin, *Ind. Eng. Chem. Res.*, 2010, **49,** 1697.
39 R. Prasher, P. Bhattacharya and P. E. Phelan, *Phys. Rev. Lett.*, 2005, **94,**
40 J. Koo and C. Kleinstreuer, *J. Nanopart. Res.*, 2005, **7,** 324.
41 S. Lee, S. U. S. Choi, S. Li and J. A. Eastman, *J. Heat Trans.-T. ASME*, 1999, **121,** 280.
42 R. Prasher, D. Song, J. Wang and P. Phelan, *Appl. Phys. Lett.*, 2006, **89,** 133108.
43 S. Halelfadl, T. Maré and P. Estellé, *Exp. Therm. Fluid Sci.*, 2014, **53,** 104.
44 E. V. Timofeeva, J. L. Routbort and D. Singh, *J. Appl. Phys.*, 2009, **106**, 014304.